Int J Clin Exp Pathol 2017;10(2):1519-1528
www.ijcep.com /ISSN:1936-2625/IJCEP0043670

Original Article

The value of performing dual-source dual-energy computed tomography in analysis strategy for urinary mixed stone

Xiao-Gang Wang[1*], Bo Fan[1*], Wei Wang[1], Yi-Ying Jin[1], Yan Jin[2], Zhi-Qiang Yang[3], Xian-Cheng Li[1,4]

[1]*Department of Urology, The Second Affiliated Hospital of Dalian Medical University, Dalian, Liaoning, China; Departments of* [2]*Laboratory Medicine,* [3]*Cardiac Imaging,* [4]*Urology, The First Affiliated Hospital of Dalian Medical University, Dalian, Liaoning, China.* [*]*Equal contributors.*

Received November 6, 2016; Accepted November 21, 2016; Epub February 1, 2017; Published February 15, 2017

Abstract: The aim of this study was to characterize and explore the mixed urinary stones by using Dual-Source Dual-Energy Computed Tomography (DSDECT) in vitro. Study scanned 134 human pure and mixed stones that were embedded into fresh porcine kidneys. Image analysis of these stones gave us the mean attenuation values in Hounsfield units (HU) and dual-energy index (DEI) at 80 kVp and 140 kVp. The mean of attenuation values, dual-energy and DEI were statistically different between uric acid (UA) containing and other stones, including mixed stones. For mixed stone, COX/UA and COX/PH had significantly difference in DEI ($P<0.05$), and the HU of 80 kVp, 140 kVp, and dual-energy were significantly different among COX/PH and PH/UA groups. The 80 kVp HU, 140 kVp HU and dual energy HU were significantly higher in COX/PH group compared with PH/UA group (1316.31 vs 813.23, 717.60 vs 440.03, 951.49 vs 557.38, respectively).The value of 80 kVp HU, 140 kVp HU and dual energy HU in COX/UA was 1052.54, 704.12, 802.94 respectively. DSDECT was precise in the differentiation of UA-containing stones and gave promising results for mixed stones of different types.

Keywords: Dual-source dual-energy computed tomography, urinary stone, stone composition

Introduction

Urinary calculi is a worldwide disease with an increasingly morbidity and a high recurrence rate. Incidence of urinary calculi is up to 1~5% in China; it could be even higher in some special area [1]. The following factors contribute to the etiopathogenesis and development of urinary calculi: (*a*) congenital factors, such as sex and age [2]; (*b*) dietary factors [3]; (*c*) abnormal factors, such as metabolic disorder (hypercalcemia or hyperoxaluria), urinary tract obstruction and urinary tract infection [4]; and (*iv*) genetic and geographic factors [2-5].

Although patient's symptoms and stone size are two important factors for selection of appropriate treatment options, knowledge of chemical composition of the stone would be crucial to determine the optimal management, assess the effectiveness of therapy, and formulate strategies to prevent recurrence [6-8]. In the case of calcareous stones (calcium oxalate calculus or calcium phosphate calculus), the treatment may require surgical intervention with shock wave lithotripsy (SWL), ureteroscopy or percutaneous nephrolithotomy (PCNL), and not adjunct medical therapy [9, 10]. In the case of non-calcareous stones, the treatment typically includes adjunct medical therapy that is also different according to the characteristics of each stone type. For example, UA-containing calculus may be treated with urinary alkalinization and low purine diet; and patients with struvite stones will often be treated with antibiotics before intervention [11-13]. The recent advances in computed tomography (CT) attracted attention of the urologists and radiologists [14] that led to the progress in the management of 10% to 25% patients after reliable identification of stone composition [15].

With the CT development, the sensitivity of dual-energy spectral imaging is increased. This novel technology utilizes two x-ray tubes (80 kilovoltage and 140 kilovoltage) for image col-

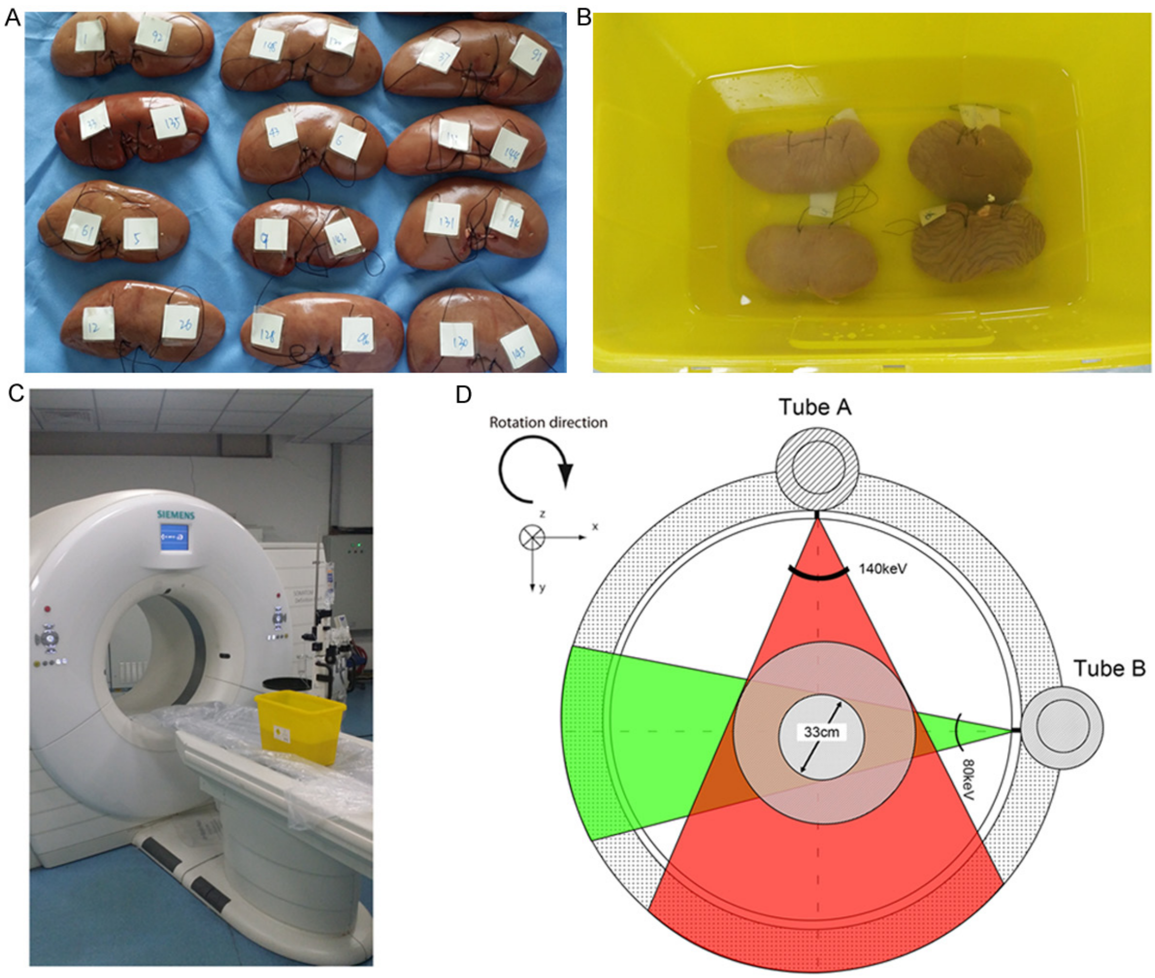

Figure 1. Study Design All human urinary stones were embedded into fresh porcine kidneys (A) and then the kidneys were placed in a 20-cm-deep water phantom (B). Water phantom was scanned with DSDECT (C) using 2 x-ray tubes arranged at an angle of 90° (D).

lection. When image is collected at low and high-energy x-ray spectra, it has different attenuation values that allow to detect different materials [16, 17]. Several studies on the predictive power of dual-energy CT (DECT) for analysis of pure stones have been recently published [16, 18, 19]. However, there is a lack of information about the predictive power of DSDECT for mixed stones. In this work, we used DSDECT to explore the characteristics of mixed urinary stones *in vitro* and to develop criteria for distinguishing of different types of stones.

Materials and methods

Study design and patients

We performed a study with 212 urinary calculi obtained from the sample bank of The First Affiliated Hospital of Dalian Medical University and The Second Affiliated Hospital of Dalian Medical University. These samples have been collected during surgical and endoscopic interventions between December 2007 and June 2015. The stone's diameter ranged from 0.1 to 6.3 cm (the mean size was 1.4 cm). After exclusion of the stones with a diameter less than 4 mm (stones of this size usually is ejected spontaneously and without treatment) [20], we obtained a dataset of 134 stones.

The stone's composition was determined by two doctors of laboratory medicine (YJ, WW) using chemical process [21] which was a traditional method still used in this region. The stones were classified according to their predominant component. The following groups were identified in our sample bank: uric acid (UA), calcium oxalate (COX), phosphate (PH), carbonate (CAR), calcium oxalate and uric acid (COX/UA), phosphate and uric acid (PH/UA),

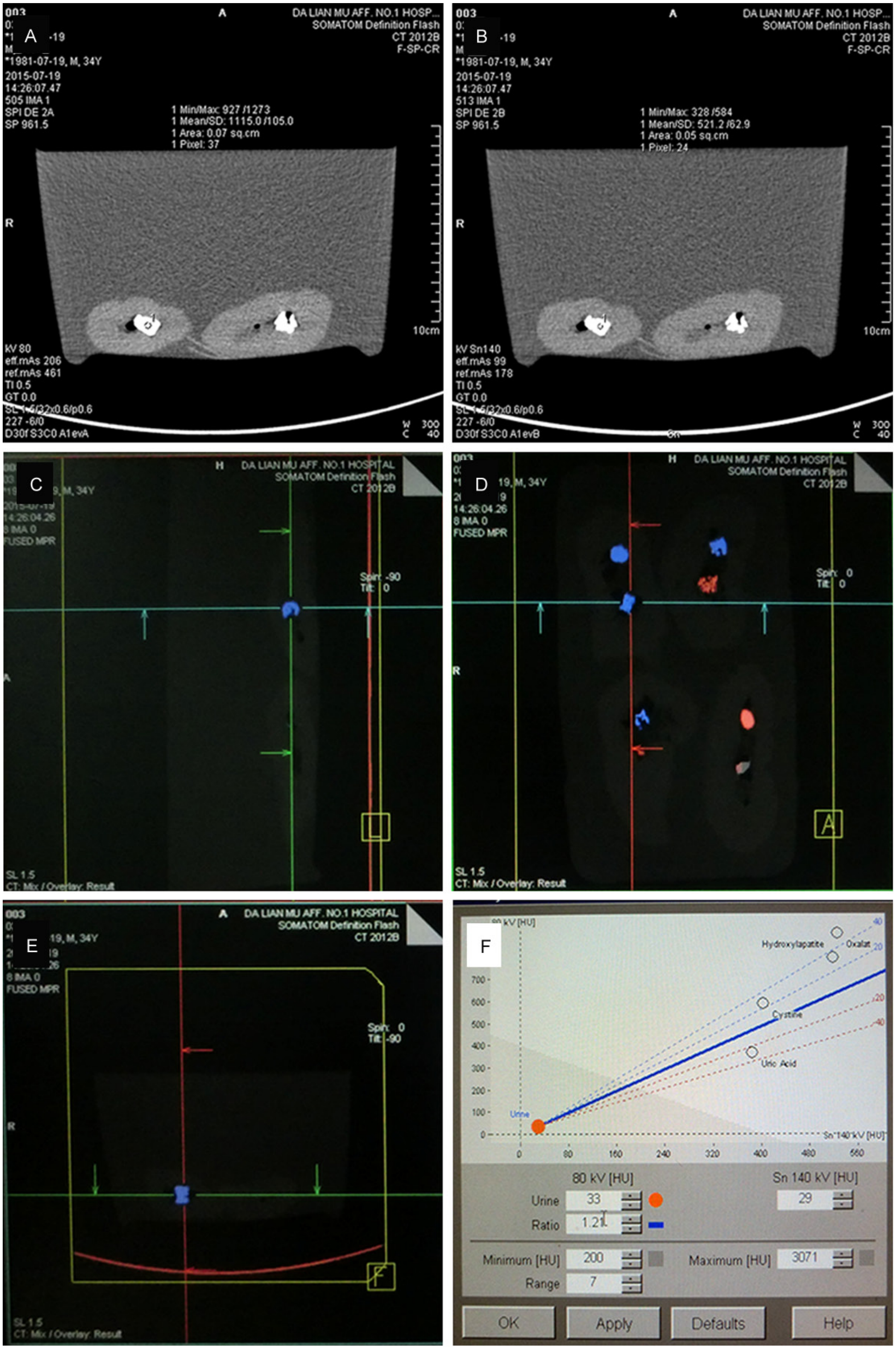
A
DA LIAN MU AFF. NO.1 HOSP...
SOMATOM Definition Flash
1 Min/Max: 927 /1273
1 Mean/SD: 1115.0 /105.0
1 Area: 0.07 sq.cm
1 Pixel: 37
kV 80
B
DA LIAN MU AFF. NO.1 HOSP...
SOMATOM Definition Flash
1 Min/Max: 328 /584
1 Mean/SD: 521.2 /62.9
1 Area: 0.05 sq.cm
1 Pixel: 24
kV Sn140
C
D
E
DA LIAN MU AFF. NO.1 HOSPITAL
SOMATOM Definition Flash
FUSED MPR
CT: Mix / Overlay: Result
F
Hydroxylapatite
Oxalat
Cystine
Uric Acid
Urine
80 kV [HU]
Sn 140 kV [HU]
Urine
Ratio
Minimum [HU]
Maximum [HU]
Range
OK
Apply
Defaults
Help

Figure 2. The image of DSDECT. Radiologists measured attenuation value in image at 80 kVp (A) and 140 kVp (B). Three images of stones in sagittal (C), coronal (D), and axial planes (E) and settings dialog (F). In diagram, four stone types (calcium oxalate, hydroxyapatite, cystine, and uric acid) are described by four small circles (CT density at 140 kVp on x-axis and CT density at 80 kVp on y-axis). Blue line splits plane in two parts: uric acid (red) and nouric acid (blue).

Table 1. Characteristics of patients and stones

Mean stone size ± SD cm	1.4±1.1 (0.1-6.3)		
Stone location	Bladder stone	49	19%
	Kidney stone	133	65%
	Ureteral stone	30	16%
Sex	Male	124	58%
	Female	88	42%
Age	5-87		

carbonate, phosphate and uric acid (CAR/PH/UA), calcium oxalate, phosphate and uric acid (COX/PH/UA), calcium oxalate and phosphate (COX/PH), carbonate and phosphate (CAR/PH) containing stones.

All stones were embedded into fresh porcine kidneys (obtained from a slaughterhouse) after hydrating in distilled water for 24 hours. The incision of the stones was coronal and implantation was performed in a water bath to keep air bubbles from entering into the collecting system. The location of each stone embedded in the kidneys was marked. The kidneys were placed in a 20-cm-deep water phantom and then scanned (**Figure 1**).

Dual-Source Dual-Energy Computed Tomography (DSDECT)

All examinations were performed with a DSDECT device (Somatom Definition, Siemens Healthcare). Technical parameters for the dual-energy scan were as follows: tube voltage, 80 kVp and 140 kVp; reference tube current, 96 mA and 400 mA with automatic exposure control; acquisition slice thickness, 5 mm; reconstruction slice thickness, 1.5 mm; reconstruction increment, 1.5 mm; gantry rotation time, 0.5 second; filter kernel, B30f (medium smooth); and detector configuration, 32 × 0.6 mm. Image analysis was performed by two independent radiologists (ZQY, WW) who had years of experience in abdominal imaging and were blinded to the stone composition (**Figure 2**). The readout was carried out on a dedicated remote workstation (Leonardo, Siemens Healthcare) with a commercial software set (Syngo Dual Energy Viewer, Siemens Healthcare). Regions of interest (ROI) of measured attenuation value for each urinary stone were detected with the software mentioned above. The dual-energy index (DEI) [22] was calculated from DECT data (80/140 kVp), according to the following formula:

$$DEI = \frac{\text{CT number (80 kVp)} - \text{CT number (140 kVp)}}{\text{CT number (80 kVp)} + \text{CT number (140 kVp)} + 2000}$$

Statistical analysis

Statistical analysis was performed using commercially available statistical software (SPSS, version 21.0, Chicago, IL). One-way ANOVA was conducted to compare the attenuation values, DEI values and overlap values among the different compositions of urinary stones. To adjust for multiplicity, Fisher's least significant difference t test correction was used when multiple comparisons were performed. Pearson correlation was used to analyze attenuation values and mixed stone sizes. Samples were considered statistically different, if P value was <0.05.

Results

Urinary stones were obtained from the 212 patients during surgical or endoscopic interventions. Characteristics of patients and stones are shown in **Table 1**.

For pure stones, chemical analysis revealed 56 (42%) COX, 37 (27%) PH, 40 (30%) UA, 1 (1%) CAR stones (**Figure 3A**). For mixed stones, it revealed 34 (44%) COX/PH, 26 (33%) COX/UA, 12 (15%) PH/UA, 3 (4%) CAR/PH, 2 (3%) COX/PH/UA, 1 (1%) CAR/PH/UA stones (**Figure 3B**).

The DSDECT software displayed pure uric acid stone in a red color and non-uric acid stone in a blue color (**Figure 2**). All mixed stones were displayed in a blue color. The results of the quantitative image analysis for pure stones are shown in **Table 2**. The attenuation value, dual energy and DEI were significantly different between UA-containing and other stones, including mixed stones (P<0.05). The mixed stones, COX/UA and COX/PH, had statistically significant difference (P<0.05) in DEI and attenuation values. The dual energy were statistically different

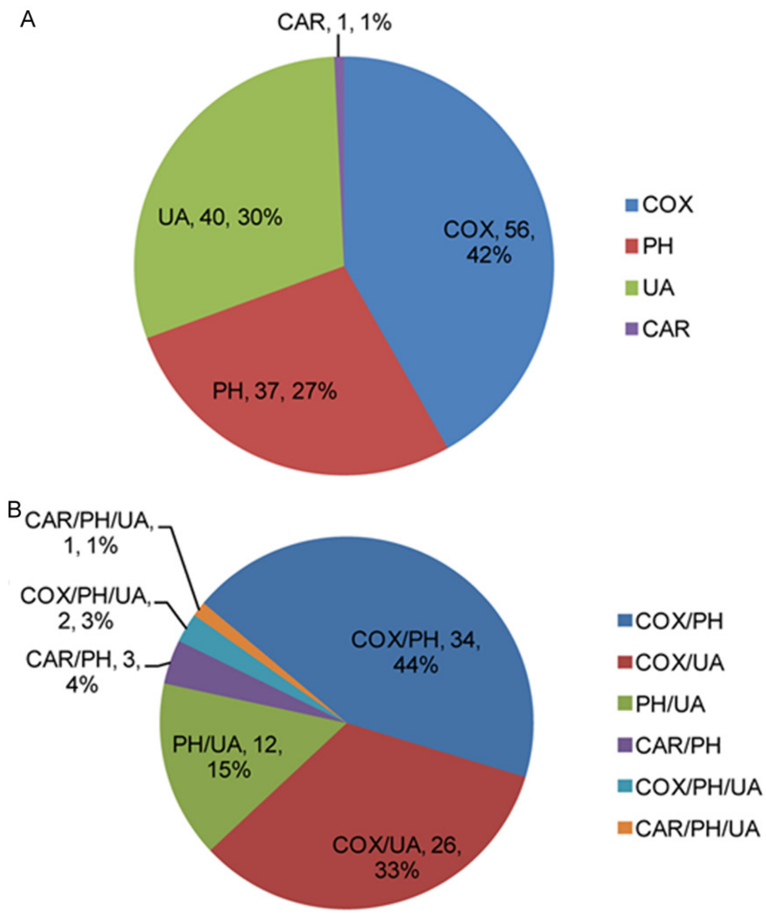

Figure 3. Distribution of mineral composition of pure stones (A) and mixed stones (B).

among COX/PH and PH/UA groups. The 80 kVp HU, 140 kVp HU and dual-energy HU were significantly higher in COX/PH group compared with PH/UA group (1316.31 vs 813.23, 717.60 vs 440.03, 951.49 vs 557.38, respectively). The value of 80 kVp HU, 140 kVp HU and dual-energy HU in COX/UA was 1052.54, 704.12, 802.94 respectively. The date are summarized in the **Table 3**. Mixed stones did not show a correlation between size and attenuation value overall, but it may have such tending (**Figure 4**).

Discussion

Nowadays, urinary stone disease has been an increasing problem. The choice of method for the clinical treatment of urinary tract stones depends not only on stone size, location, and brittleness, but also on stone composition [23]. Therefore, the ability to predict stone composition before the treatment is a crucial feature for the selection of an optimal treatment. During the past few years, there were several studies to achieve this aim using conventional CT, which are widely used in current clinical practice. Initially reported in 1995 [24], the sensitivity and specificity of helical CT for diagnosis of urinary calculi was 95%-98% and 96%-100% respectively [25, 26]. However, the usage of CT for the identification of the chemical composition of the urinary stones has been questioned due to some contradictory results. Motley et al described that UA-containing stones could be distinguished from calcium stones, but the mean attenuation values were not predictable after including struvite and cysteine stones [27]. Furthermore, the accurate identification were precluded by overlap of their attenuation value ranges [27]. Although an *in vitro* study by Deveci et al demonstrated that the chemical compositions of both pure and mixed stone types could be determined accurately by attenuation value, the application of their method in an *in vivo* cohort is still not clear [28].

The application of energy information in DECT imaging has become a popular area of research with the development of radiological technology. There are two main DECT types, such as a dual-source DECT and single-source DECT. The single-source DECT relies on fast kilovoltage switching and a single-source dual-energy scanner with dual detector layers. Most of the studies are based on the application of dual-source DECT. Each material has a specific change in attenuation between images with a high-energy spectrum and with a low-energy spectrum.

This attenuation differentiates one type stone from the others with a nuanced characterization. DSDECT has two separate x-ray tubes that can be operated at two different tube potentials. DSDECT's two separate detectors can

Table 2. 80 kVp HU, 140 kVp HU, DEI, overlap value and dual-energy HU from pure stones

Hounsfield unit variable	COX (n=34)		UA (n=33)		PH (n=26)		UA vs COX	UA vs PH	PH vs COX
	Mean ± SD	Range	Mean ± SD	Range	Mean ± SD	Range		*P* Value	
80 kvp	1236.26±496.62	1062.99 to 1409.54	442.75±188.27	376.01 to 509.49	1233.47±470.31	1033.50 to 1413.44	<0.05	<0.05	0.906
140 kvp	704.12±259.86	550.94 to 748.78	423.28±132.71	550.94 to 748.78	649.86±244.91	550.94 to 748.78	<0.05	<0.05	0.363
DEI	0.238±0.118	0.196 to 0.297	0.009±0.092	-0.023 to 0.042	0.272±0.067	0.245 to 0.299	<0.05	<0.05	0.132
Overlap	100.02±126.01	56.05 to 143.99	-14.18±16.64	-21.08 to -8.27	76.37±23.44	66.90 to 85.83	<0.05	<0.05	0.174
Dual-Energy	889.32±352.71	766.25 to 1012.39	404.23±137.12	355.61 to 452.85	819.57±321.01	689.91 to 949.23	<0.05	<0.05	0.381

Table 3. 80 kVp HU, 140 kVp HU, DEI, overlap value and dual-energy HU from mixed stones

Hounsfield unit variable	COX/UA (n=12)		COX/PH (n=24)		PH/UA (n=5)		COX/UA vs COX/PH	COX/PH vs PH/UA	COX/UA vs PH/UA
	Mean ± SD	Range	Mean ± SD	Range	Mean ± SD	Range		*P* Value	
80 kvp	1052.54±340.18	1110.48 to 1522.13	1316.31±487.43	1110.48 to 1522.13	813.23±314.78	422.37 to 1024.09	0.074	<0.05	0.280
140 kvp	627.51±201.25	544.64 to 800.38	717.60±281.81	598.61 to 836.60	440.03±167.88	231.57 to 648.49	0.577	<0.05	0.058
DEI	0.187±0.085	0.133 to 0.241	0.267±0.054	0.244 to 0.290	0.251±0.055	0.182 to 0.319	<0.05	0.707	0.181
Overlap	55.00±19.71	42.47 to 67.53	85.72±22.98	76.02 to 95.43	80.76±22.82	52.42 to 109.10	0.193	0.880	0.468
Dual-Energy	802.94±244.54	647.57 to 958.32	951.49±410.37	778.20 to 1124.78	557.38±115.01	414.47 to 700.29	0.170	<0.05	0.132

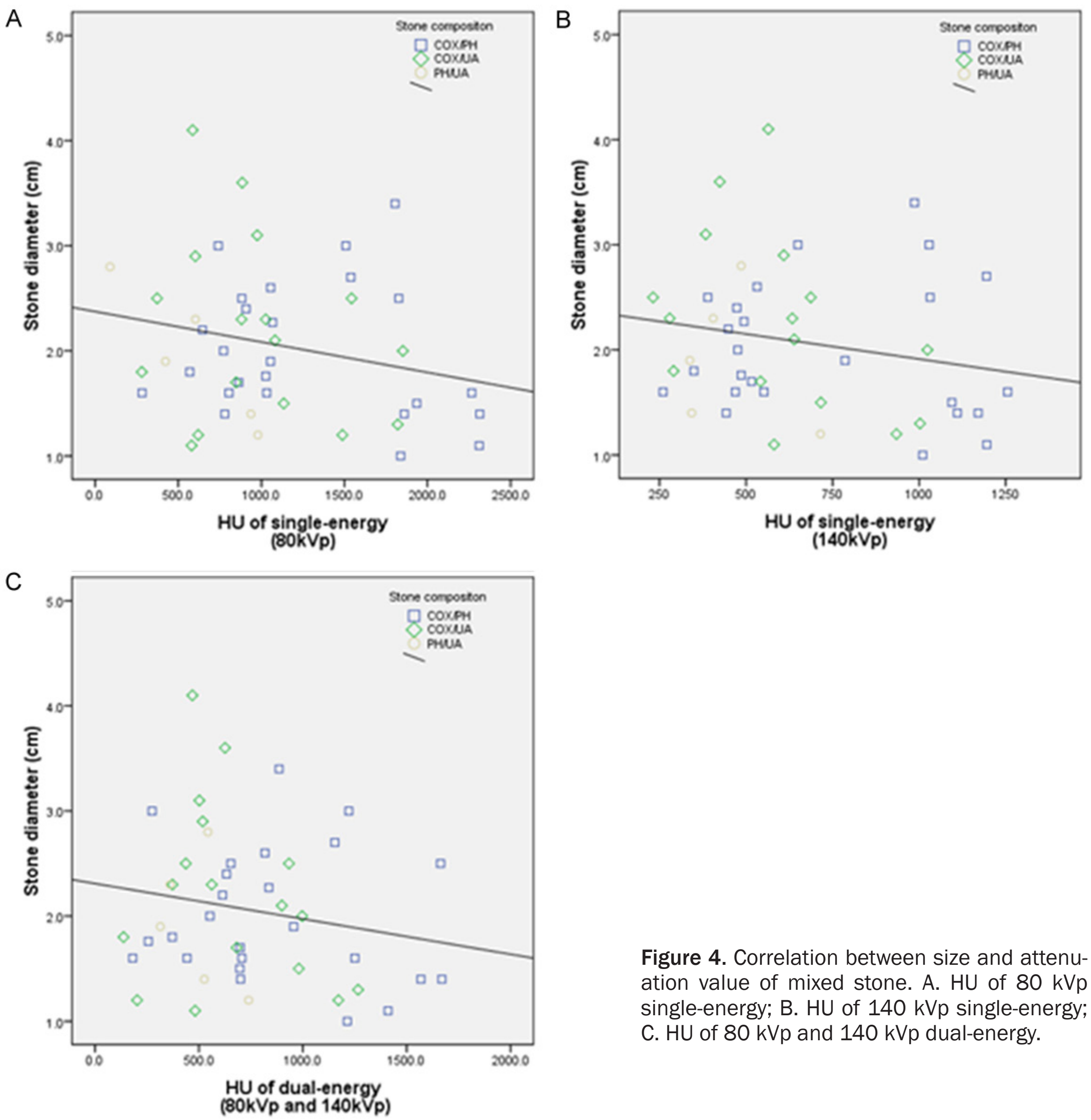

Figure 4. Correlation between size and attenuation value of mixed stone. A. HU of 80 kVp single-energy; B. HU of 140 kVp single-energy; C. HU of 80 kVp and 140 kVp dual-energy.

acquire two different image datasets. Low-energy scans can be obtained at 80 or 100 kVp simultaneously, and high-energy scans can be obtained at 120 or 140 kVp. DSDECT can optimize image quality because the capacity of its two separate x-ray sources allows beam filtration and adjustment of the current in each tube.

In recent years, DECT with either a single or dual x-ray tube had advances in determination of the stone composition. Qu et al improved separation in CT number ratio between the five stone groups (uric acid, cystine, struvite, calcium oxalate, carbonate apatite and hydroxyapatite) using 128-slice DSDECT scanner [29]. DSDECT was successfully used by Manglaviti et al for prediction of three types of stone, such as calcium oxalate-, cysteine- and uric acid-containing stones [20]. In addition, Li et al [16] found that the differences in mean of calcium density, calcium-water ratio, and radiodensity were statistically significant among five groups (uric acid, struvite, cystine, calcium phosphate and calcium oxalate) and demonstrated dual energy spectral CT provides a novel method for better characterization of pure urinary stones.

Although the studies which applied DECT to predict stone composition were gradually increasing, most of them were focused on the predictive power of DECT for analysis of pure stones [16, 30-32]. The increased appearance of mixed stones in clinic requires the development of the reliable methods for the detection of these stones in vivo. In our study, we analyzed the composition of mixed stones using DSDECT and distinguished COX/UA and COX/PH groups, as well as COX/PH and PH/UA groups. We speculated that uric acid might play an important role in this differentiation, because uric acid stones are made of low molecular weight compound and they have a higher attenuation value at higher voltages. However, other stones containing calcium oxalate, phosphate or cystine are made of high-molecular-weight compounds and have a higher HU value at lower voltages. In a result, uric acid mixed stones containing uric acid can be easily differentiated. However, we found that we cannot distinguish PH/UA and COX/UA stones by our method. The patients with both these stone types, PH/UA and COX/UA, can have with urinary alkalization or allopurinol therapy before subsequent PCNL or extracorporeal SWL.

The relation between attenuation value of stones and effectiveness of chosen treatment (PCNL/SWL) were analyzed in several studies. Michio Tanaka's study indicated that stone's attenuation value less than 780 HU might have a successful result on SWL treatment. The combination of stone cross-sectional area and stone attenuation value was useful in determining the SWL treatment for patients with urinary calculi [33]. Kawahara et al showed that stones with higher CT densities are more resistant to ESWL than those with lower CT densities [34]. There was no high HU threshold above which clinicians would not consider SWL as a treatment option for urinary stones [33, 35, 36]. Largo et al reported that stones' HU/DEI ratio was a significant and independent predictor for extracorporeal SWL in the number of required shock waves [35]. At the same time, Gucuk et al indicated that the attenuation value was one of independent predictors of the failure of the PCNL. The cut-off value was 677.5, and having a HU value under the cut-off value increased the likelihood of procedure failure by 2.65 times [37]. According to above studies, we could consider that stones with low HU value were advantageous to extracorporeal SWL compared with PCNL. In our study, PH/UA stones have lowest HU value, suggesting that patients with PH/UA will have a better result when treated with extracorporeal SWL rather than PCNL.

Several limitations of the present study should be considered. Although COX and PH had been identified by DSDECT, COX contained calcium oxalate monohydrate and calcium oxalate dehydrate. Meanwhile, subtypes of PH were made of struvite, brushite and calcium phosphate. It suggested that further investigations will be required to differentiate subtypes of calcium stones. Moreover, a receiver operating characteristic study were not performed to establish a threshold for sensitivity and specificity, as the sample size of each mixed stone group (such as PH/UA and COX/UA) was small. Large-scale studies in the future are required to establish the threshold values for quantitative evaluation of the stone types. In addition, the measurements of stones performed *in vitro* could give inaccurate results in comparison with measurements performed *in vivo.* Phantoms may not accurately reflect the anatomic surroundings of renal stones. Future studies with a larger sample size should include *in vivo* study to determine clinical usefulness.

Conclusion

DSDECT differentiates uric and non-uric acid-containing stones, and also allows analysis of characteristics among mixed stones. It offers us a chance to make a better treatment plan for the patients with urinary stone disease.

Acknowledgements

This work was partly supported by the Natural Science Foundation of China (code 81572505).

Disclosure of conflict of interest

None.

Address correspondence to: Dr. Xian-Cheng Li, Department of Urology, The Second Affiliated Hospital of Dalian Medical University, Shahekou District Zhongshan Road no. 467 of Dalian, Liaoning, China. Tel: 0086-0411-84671291; Fax: 0086-0411- 84671291; E-mail: xiancheng_li@sina.cn

References

[1] Zeng G, Mai Z, Zhao Z, Li X, Zhong W, Yuan J, Wu K, Wu W. Treatment of upper urinary calculi with Chinese minimally invasive percutaneous nephrolithotomy: a single-center experi-

ence with 12,482 consecutive patients over 20 years. Urolithiasis 2013; 41: 225-229.
[2] Moe OW. Kidney stones: pathophysiology and medical management. Lancet (London, England) 2006; 367: 333-344.
[3] Ferraro PM, Curhan GC, Gambaro G, Taylor EN. Total, Dietary, and Supplemental Vitamin C Intake and Risk of Incident Kidney Stones. Am J Kidney Dis 2016; 67: 400-7.
[4] Astroza GM, Neisius A, Tsivian M, Preminger GM, Lipkin ME. Treatment Response in Stone Patients with Low Urinary pH and Hypocitraturia Stratified by Body Mass Index. J Urol 2016; 195: 653-7.
[5] Skolarikos A, Straub M, Knoll T, Sarica K, Seitz C, Petřík A, Türk C. Metabolic evaluation and recurrence prevention for urinary stone patients: EAU guidelines. Eur Urol 2015; 67: 750-763.
[6] Wiener SV, Deters LA, Pais VM Jr. Effect of stone composition on operative time during ureteroscopic holmium: yttrium-aluminum-garnet laser lithotripsy with active fragment retrieval. Urology 2012; 80: 790-794.
[7] Ramaswamy K, Killilea DW, Kapahi P, Kahn AJ, Chi T, Stoller ML. The elementome of calcium-based urinary stones and its role in urolithiasis. Nat Rev Urol 2015; 12: 543-557.
[8] Scherer K, Braig E, Willer K, Willner M, Fingerle AA, Chabior M, Herzen J, Eiber M, Haller B, Straub M, Schneider H, Rummeny EJ, Noël PB, Pfeiffer F. Non-invasive differentiation of kidney stone types using X-ray dark-field radiography. Sci Rep 2015; 5: 9527.
[9] Holmes RP, Knight J, Assimos DG. Lowering urinary oxalate excretion to decrease calcium oxalate stone disease. Urolithiasis 2016; 44: 27-32.
[10] Orhan N, Onaran M, Şen İ, Işık Gönül İ, Aslan M. Preventive treatment of calcium oxalate crystal deposition with immortal flowers. J Ethnopharmacol 2015; 163: 60-67.
[11] Joshi HB, Kumar PV, Timoney AG. Citric acid (solution R) irrigation in the treatment of refractory infection (struvite) stone disease: is it useful? Eur Urol 2001; 39: 586-590.
[12] Friedlander JI, Moreira DM, Hartman C, Elsamra SE, Smith AD, Okeke Z. Comparison of the metabolic profile of mixed calcium oxalate/uric acid stone formers to that of pure calcium oxalate and pure uric acid stone formers. Urology 2014; 84: 289-294.
[13] Heilberg IP. Treatment of patients with uric acid stones. Urolithiasis 2016; 44: 57-63.
[14] Ngo TC, Assimos DG. Uric Acid nephrolithiasis: recent progress and future directions. Rev Urol 2007; 9: 17-27.
[15] Kulkarni NM, Eisner BH, Pinho DF, Joshi MC, Kambadakone AR, Sahani DV. Determination of renal stone composition in phantom and patients using single-source dual-energy computed tomography. J Comput Assist Tomogr 2013; 37: 37-45.
[16] Li X, Zhao R, Liu B, Yu Y. Gemstone Spectral Imaging Dual-energy Computed Tomography: A Novel Technique to Determine Urinary Stone Composition. Urology 2013; 81: 727-730.
[17] Duan X, Li Z, Yu L, Leng S, Halaweish AF, Fletcher JG, McCollough CH. Characterization of Urinary Stone Composition by Use of Third-Generation Dual-Source Dual-Energy CT With Increased Spectral Separation. AJR Am J Roentgenol 2015; 205: 1203-1207.
[18] Wisenbaugh ES, Paden RG, Silva AC, Humphreys MR. Dual-energy vs Conventional Computed Tomography in Determining Stone Composition. Urology 2014; 83: 1243-1247.
[19] Selby MG, Vrtiska TJ, Krambeck AE, McCollough CH, Elsherbiny HE, Bergstralh EJ, Lieske JC, Rule AD. Quantification of asymptomatic kidney stone burden by computed tomography for predicting future symptomatic stone events. Urology 2015; 85: 45-50.
[20] Manglaviti G, Tresoldi S, Guerrer CS, Di Leo G, Montanari E, Sardanelli F, Cornalba G. In Vivo Evaluation of the Chemical Composition of Urinary Stones Using Dual-Energy CT. AJR Am J Roentgenol 2011; 197: W76-W83.
[21] Ye YW. Clincial Laboratory Diagnostics. People's Medical Publishing House; 1989.
[22] Graser A, Johnson TR, Bader M, Staehler M, Haseke N, Nikolaou K, Reiser MF, Stief CG, Becker CR. Dual energy CT characterization of urinary calculi: initial in vitro and clinical experience. Invest Radiol 2008; 43: 112-119.
[23] Li XH, Zhao R, Liu B, Yu YQ. Determination of urinary stone composition using dual-energy spectral CT: Initial in vitro analysis. Clin Radiol 2013; 68: e370-e377.
[24] Smith RC, Rosenfield AT, Choe KA, Essenmacher KR, Verga M, Glickman MG, Lange RC. Acute flank pain: comparison of non-contrast-enhanced CT and intravenous urography. Radiology 1995; 194: 789-794.
[25] Fielding JR, Silverman SG, Samuel S, Zou KH, Loughlin KR. Unenhanced helical CT of ureteral stones: a replacement for excretory urography in planning treatment. AJR Am J Roentgenol 1998; 171: 1051-1053.
[26] Hamm M, Wawroschek F, Weckermann D, Knöpfle E, Häckel T, Häuser H, Krawczak G, Harzmann R. Unenhanced helical computed tomography in the evaluation of acute flank pain. Eur Urol 2001; 39: 460-465.
[27] Motley G, Dalrymple N, Keesling C, Fischer J, Harmon W. Hounsfield unit density in the determination of urinary stone composition. Urology 2001; 58: 170-173.

[28] Deveci S, Coşkun M, Tekin MI, Peşkircioglu L, Tarhan NC, Ozkardeş H. Spiral computed tomography: role in determination of chemical compositions of pure and mixed urinary stones--an in vitro study. Urology 2004; 64: 237-240.

[29] Qu M, Ramirez-Giraldo JC, Leng S, Williams JC, Vrtiska TJ, Lieske JC, McCollough CH. Dual-Energy Dual-Source CT With Additional Spectral Filtration Can Improve the Differentiation of Non–Uric Acid Renal Stones: An Ex Vivo Phantom Study. Am J Roentgenol 2011; 196: 1279-1287.

[30] Stewart G, Johnson L, Ganesh H, Davenport D, Smelser W, Crispen P, Venkatesh R. Stone Size Limits the Use of Hounsfield Units for Prediction of Calcium Oxalate Stone Composition. Urology 2015; 85: 292-295.

[31] Hidas G, Eliahou R, Duvdevani M, Coulon P, Lemaitre L, Gofrit ON, Pode D, Sosna J. Determination of renal stone composition with dual-energy CT: in vivo analysis and comparison with x-ray diffraction. Radiology. 2010; 257: 394-401.

[32] Torricelli FC, Marchini GS, De S, Yamaçake KG, Mazzucchi E, Monga M. Predicting urinary stone composition based on single-energy noncontrast computed tomography: the challenge of cystine. Urology 2014; 83: 1258-1263.

[33] Tanaka M, Yokota E, Toyonaga Y, Shimizu F, Ishii Y, Fujime M, Horie S. Stone attenuation value and cross-sectional area on computed tomography predict the success of shock wave lithotripsy. Korean J Urol 2013; 54: 454-459.

[34] Kawahara T, Miyamoto H, Ito H, Terao H, Kakizoe M, Kato Y, Ishiguro H, Uemura H, Yao M, Matsuzaki J. Predicting the mineral composition of ureteral stone using non-contrast computed tomography. Urolithiasis 2016; 44: 231-9.

[35] Largo R, Stolzmann P, Fankhauser CD, Poyet C, Wolfsgruber P, Sulser T, Alkadhi H, Winklhofer S. Predictive value of low tube voltage and dual-energy CT for successful shock wave lithotripsy: an in vitro study. Urolithiasis 2016; 44: 271-6.

[36] Wang LJ, Wong YC, Chuang CK, Chu SH, Chen CS, See LC, Chiang YJ. Predictions of outcomes of renal stones after extracorporeal shock wave lithotripsy from stone characteristics determined by unenhanced helical computed tomography: a multivariate analysis. Eur Radiol 2005; 15: 2238-2243.

[37] Gücük A, Uyetürk U, Oztürk U, Kemahli E, Yildiz M, Metin A. Does the Hounsfield unit value determined by computed tomography predict the outcome of percutaneous nephrolithotomy? J Endourol 2012; 26: 792-796.